

# Chapter 8

## Multi-source Energy Management of Maritime Grids



### 8.1 Multiples Sources in Maritime Grids

#### 8.1.1 Main Grid

The main grid plays as the main power source of land-based maritime grids since the very beginning, such as the seaports and some coastal industries. This type of maritime grids usually operates in a harbor territory and can receive electricity from the harbor city. Some equipment in those maritime grids is driven by electricity and the others may be driven by fossil fuel. Table 8.1 shows the power sources of a terminal port.

From Table 8.1, electricity, diesel, petrol and natural gas are four main power sources for a terminal port, especially the electricity and diesel, serving for most of the port-side equipment. When a seaport is less-electrified, the portion from diesel is generally higher. In recent years, the extensive electrification of seaport becomes an irreversible trend, then the electricity now has become the primary power source of a seaport. Diesel now serves for some flexible operating equipment, such as trucks and other carriers. Similar phenomena also happen in other land-based maritime grids, such as coastal factories, since when fully electrified, electricity will serve as the main energy carrier and the main grid will be the main power source.

#### 8.1.2 Main Engines

Most types of maritime grids cannot always receive power from the main grid. They mostly operate as islanded microgrids, such as island microgrids, shipboard microgrids, and various working platforms. For the island microgrids, if they cover a wide area, a small-scale or even medium-scale power plant is possible to construct,

**Table 8.1** Possible power sources for different equipment in a seaport (data from [1])

	Diesel	Petrol	Natural gas	Electricity
Ship-to shore cranes	•			•
Mobile cranes	•			•
Rail-mounted gantry	•			•
Rubber-tired gantry	•			•
Reach stackers	•			•
Straddle carriers	•			•
Lorries	•		•	•
Generators			•	
Building				•
Lighting				•
Reefer				•
Other vehicles	•	•	•	•

and this scenario is similar to the first case since the power plant can provide sufficient power support. For the other smaller cases, the main engines act as the main power sources instead, especially in the shipboard microgrids.

Generally, the main engines have four stages of development. The first stage is in 1900–1940, which is the initial stage of main engines. In 1910, the first diesel engine driven ship “Romagna” was launched. It uses two diesel engines manufactured by “Sulzer” company. Then in 1912, the first ocean cargo ship “Selandia” uses two DM8150x diesel engines manufactured by “B&M”. In this stage, the main engines have the steamed ones and diesel ones. Then in 1940–1970, the development of main engines steps into the second stage, and this is the golden age of low-speed diesel engines. The power of a single air cylinder grows from 900–1030 kW in 1956 to 3400 kW in 1977. Then 1970–1990 is the third development stage of main engines. The theme of this stage is to reduce the fuel consumption rate. In this stage, the unit fuel consumption has reduced to 0.155–0.160 kg/(kWh), and the energy efficiency can be up to 55%. Then after 2000, the fourth stage, main engines become smarter and various advanced monitoring equipment is integrated to achieve automatic control.

Nowadays, main engines have different scales, from kilowatt to megawatt, which uses diesel, natural gas, ammonia, and so on. Some of them can use more than two types of fuels, referred to as “multi-fuel engines”. Currently, main engines serve as the main power sources for many maritime grids.

### 8.1.3 Battery and Fuel Cell

In Chaps. 1 and 5, the energy storage technologies into maritime grids, especially the battery, are illustrated in detail. Battery stores energy in the electrochemical form

and the battery cells are connected in series or in parallel or both to make up the desired voltage and capacity. There are currently many cases of battery integrated ships. Some of them are shown in Table 8.2. Nowadays, battery mostly serves as auxiliary equipment to shave the peak load of ships and benefit the operation of shipboard microgrid. In the future, the battery integration into maritime grids will be more convenient and the large-scale integration will be reality.

Since no combustion process, fuel cell has higher power generation efficiency than the traditional internal combustion engine, which is a promising power source technology in the future. Table 8.3 shows some cases of fuel cell integrated ships.

Both of battery and fuel cell have no combustion process, and are highly efficient, which are promising for future usages.

**Table 8.2** Cases of battery into ships

Name	Ship types	Battery capacity	References
Ampere	Ferry	1040 kWh	[2]
Norled	Ferry	1400 kWh	[3]
Puffer	Cargo ship	2400 kWh	[4]
Princess Benedikte	Cruise ship	2.6 MWh	[5]
Elektra	Hybrid ferry	1040 kWh	[6]
Tycho Brahe	Hybrid ferry	460 kWh	[7]
Deep ocean 01	OSV	2.8 MWh	[8]
Selbjørnsfjord	Cruise ship	585 kWh	[9]
Schleswig-Holstein	Cruise ship	1.6 MWh	[10]

**Table 8.3** Projects of some selected fuel cell-based ships

Ship	Power	Fuel	References
Viking Lady	330 kW	LNG	[11]
SF-Breeze	100 kW	Hydrogen	[12]
PA-X-ELL	30 kW	Methanol	[13]
MV Undine	250 kW	Methanol	[14]
US SSFC	2.5 MW	Diesel	[15]
MC-WAP	500 kW	Diesel	[16]
MS Forester	100 kW	Diesel	[17]
212 submarine U31	330 kW	Hydrogen/Methanol	[18]
212 submarine U32	240 kW	Hydrogen/Methanol	[19]
S-80 Submarine	300 kW	Ethanol	[20]

### 8.1.4 Renewable Energy and Demand Response

In Chaps. 1 and 5, renewable energy integration into maritime grids has been illustrated. The following Fig. 8.1 shows renewable energy integration into a seaport. Wind power, solar energy, and the main grid supply the energy demand of seaport. The ships can charge or use cold-ironing power when berthed in a seaport, which can be also viewed as using renewable energy for propulsion.

However, renewable energy is highly fluctuating and less controllable. In conventional operation patterns, the generation-side should follow the trend of renewable energy or renewable energy has to be curtailed [21]. To mitigate this issue, the demand-side can be adjusted to follow the trend of renewable energy, then the operating burden of the generation-side can be greatly reduced and the total system benefits can be improved.

In literature, demand-side management has been used in power system operation [22, 23], unit commitment [24], and so on. In the energy market, the demand-side management sources can be aggregated as one unit and acting as a “virtual power plant”. In maritime grids, demand-side management is used to adjust the propulsion system of AES [25]. Later in [26], demand-side management is used to mitigate the fluctuations of photovoltaic energy. Then [27] proposes a robust demand-side management method for a photovoltaic integrated AES.

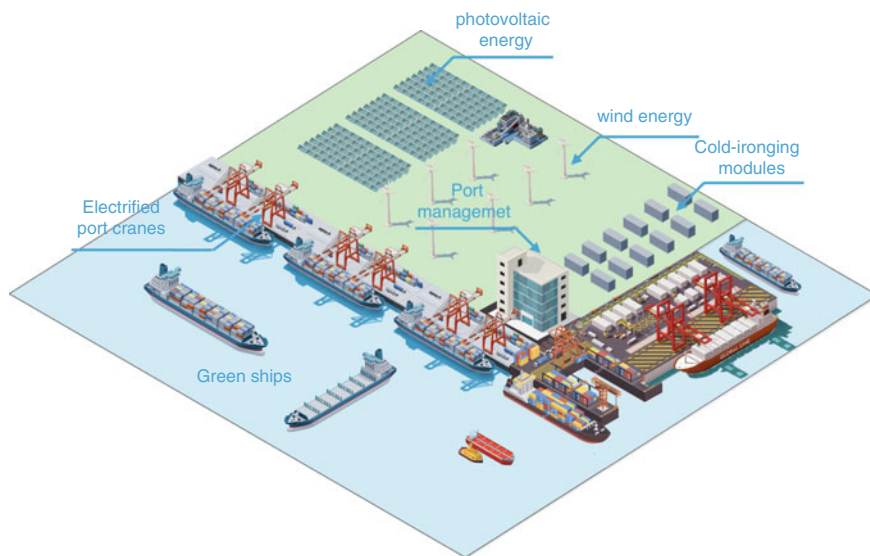


**Fig. 8.1** Renewable energy integration into a seaport

## 8.2 Coordination Between Multiple Sources in Maritime Grids

From above, maritime grids involve multiple sources, including both generation-side and demand-side, and different sources should be coordinated to achieve better system behaviors. The coordination framework is shown as the following Fig. 8.2.

From Fig. 8.2, maritime grids consist of 4 main parts, (1) generation-side, including the main grid, main engines, fuel cell, various renewables, and so on; (2) demand-side, including the propulsion in ships, and port cranes and vehicles in a seaport, and all the load demand in different platforms; (3) Energy storage, including battery, flywheel and all the energy storage technologies can be used in maritime grids, and it should be noted that energy storage can change its roles between generation-side and demand-side, i.e., it is generation-side when discharging and it is demand-side when charging; (4) Multiple networks, including electrical, heat/cooling, water, and transportation networks, and those networks are used to deliver multiple energy flows from the generation-side to the demand-side. The energy storage and networks are the interfaces between generation-side and demand-side, thus the operating strategies of them can improve the flexibility of maritime grids.

In summary, maritime grids are a series of microgrids that have specific maritime load demand, and their operation strategies can be derived from the conventional land-based microgrids while addressing some specialties.

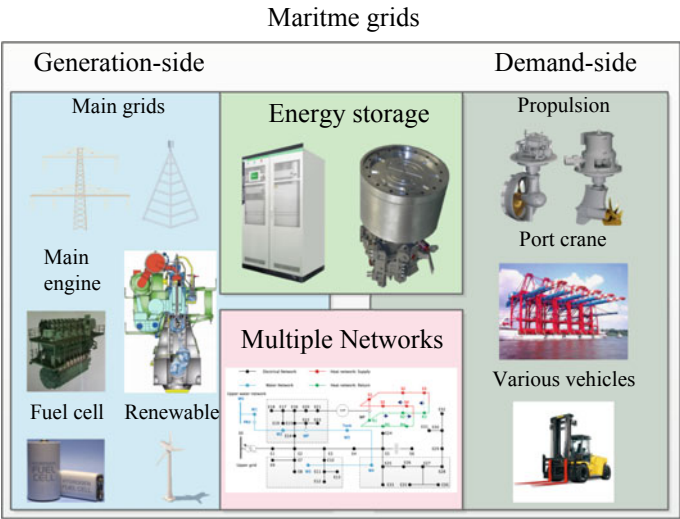


**Fig. 8.2** Coordination framework of maritime grids

### 8.3 Some Representative Coordination Cases

#### 8.3.1 Main Engine—Battery Coordination in AES

A single line diagram of AES is shown in Fig. 8.3 with two buses. 4 DGs are integrated into two buses. In this AES, bus A and bus B are both DC, and the DGs are all AC generators. The load demands include electric propellers and AC loads. Batteries are installed in two buses to act as auxiliary equipment.

Three sources are participating in the operation of AES, i.e., DGs, batteries, and the propulsion system of AES. The reason for the propulsion system to participate in demand response is shown as Fig. 8.4a, b.

In Fig. 8.4a, the propulsion load is cubically increasing with the cruising speed until the “wave wall”. In Fig. 8.4b, the constant speed and variable speed both sail 30 nm in 6 h, but they have different load curves. In this sense, the propulsion system can adjust its load demand to coordinate with the DGs and battery to facilitate the operation of AES [25] has studied this topic and the main results are shown in Fig. 8.5a, b.

From the above Fig. 8.5a, b, the coordinated adjustment of propulsion and ESS can make the operating cost and EEOI smoother since it can mitigate the peak-valley difference of onboard power demand, which proves the effects of multi-source management on AES.

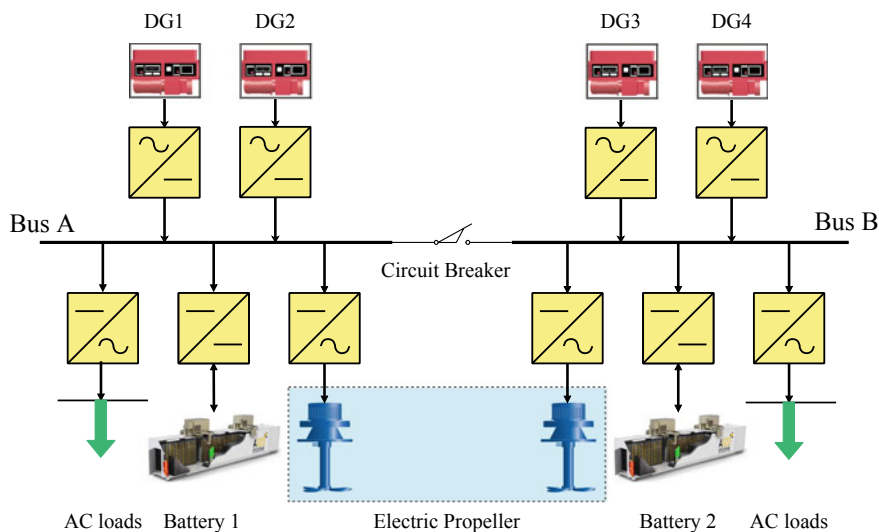


**Fig. 8.3** Single-line diagram of an AES

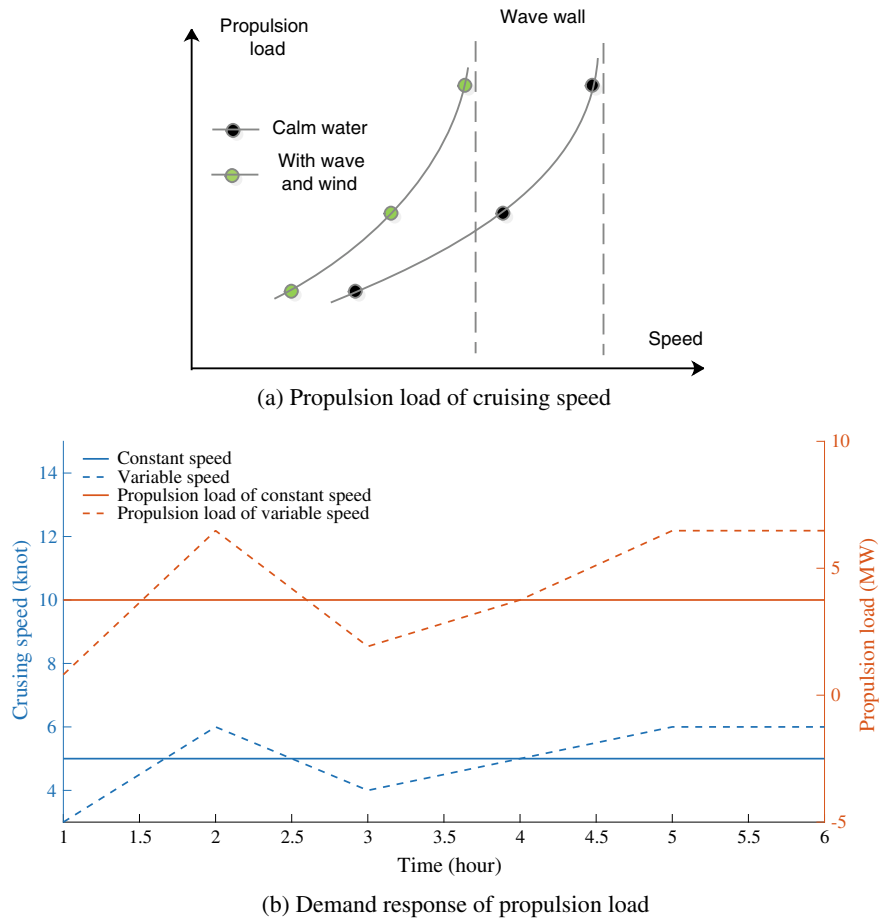


Fig. 8.4 Reason for propulsion system in demand response

8.3.2 Main Engine-Fuel Cell Coordination in AES

Compared with the main engines, fuel cell has smaller capacity and scale, which is suitable to undertake some small-scale load demands. Compared with the battery, fuel cell doesn't need charging, which can undertake long-term load demand [28] has studied this topic and compared two cases: (1) main engine; and (2) main engine-fuel cell. The testbed used in this study consists of a hybrid power source with the combined capacity of 180 kW (100 kW fuel cell, 30 kW battery, and 50 kW diesel generator). The results are shown in Fig. 8.6a, b. From the above curves, the integration of fuel cells can greatly reduce fuel consumption and CO<sub>2</sub> emission.

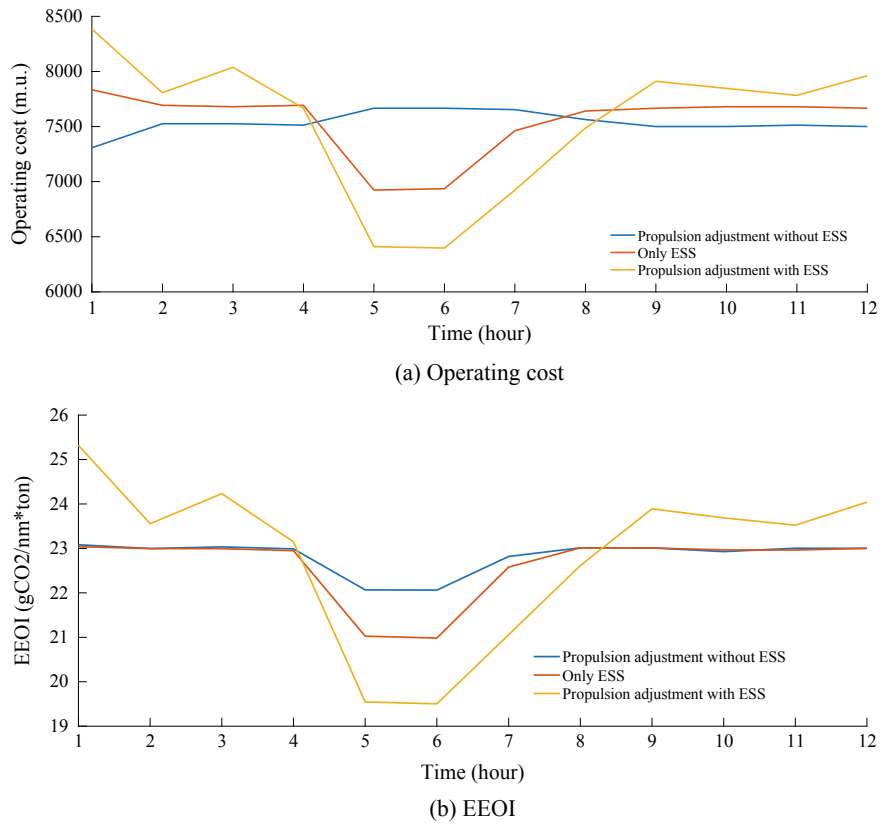


Fig. 8.5 Operating cost and EEOI with/without ESS

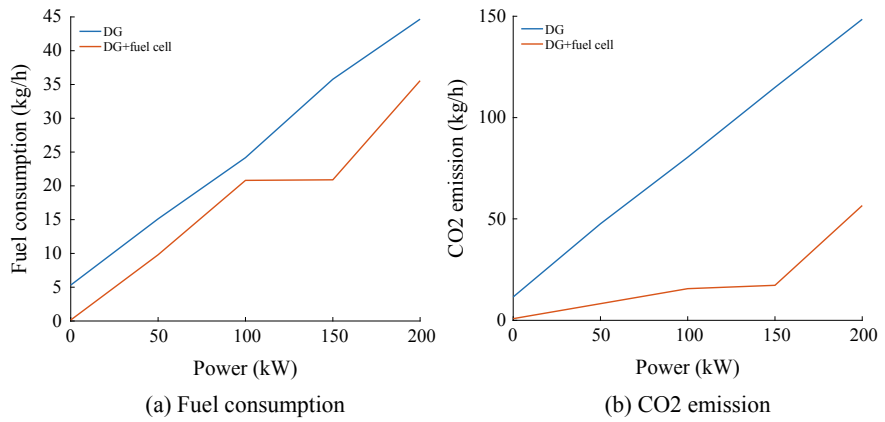


Fig. 8.6 Comparisons between DG and DG + fuel cell



8.3.3 Demand Response Coordination Within Seaports

Chapter 6 has illustrated the operation steps of quay crane (QC). Original Fig. 6.10 is now re-drawn as Fig. 8.7 below. A typical working process of a port crane includes (1) hoist, or beginning to lift up; (2) lifting up speedily; (3) lifting up speedily and the trolley moving forward; (4) lifting up with the full speed and the trolley moving forward; (5) lifting up with slowing speed and the trolley moving with full speed; (6) the trolley moving with slowing speed; (7) lifting down speedily and the trolley moving with slowing speed; (8) settling down. Step (2) and (3) usually have the biggest power demand whereas steps (6), (7) and (8) have smaller power demands.

Chapter 6 shows the integration of ESS can recover energy when lifting down the cargo. This Chapter proposes the demand response model of port crane. The dimension of QC, cargo speed, and QC power are shown in the sub-figures in Fig. 8.8. Based on Fig. 8.8, the entire lifting cargo distance is calculated as (8.1).

$$L = h_3 + (d_1 + d_2) / 2 + (h_1 + h_2) / 2 \tag{8.1}$$

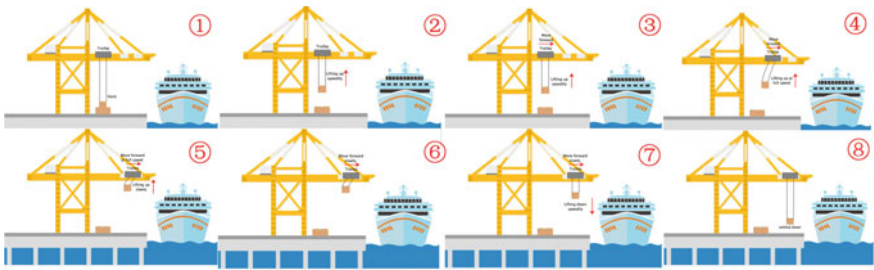


Fig. 8.7 Typical working steps for a port crane

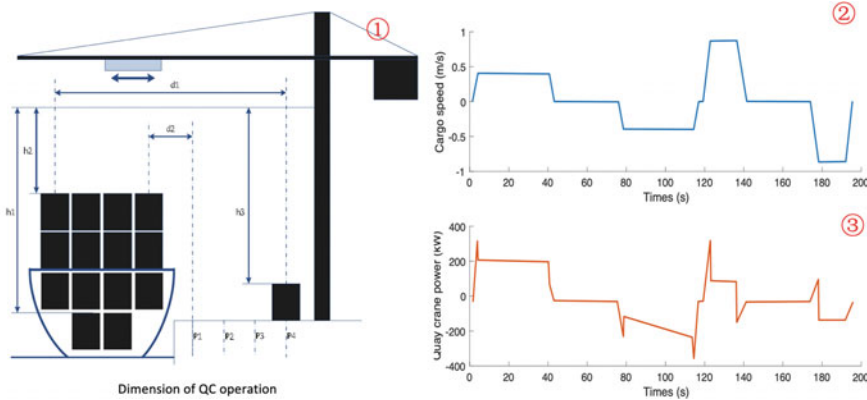


Fig. 8.8 Operation process of quay crane (QC)

From sub-figure ① and ②, the cargo speed and consumed power has a nearly linear relationship and can be shown as (8.2).

$$P = k \cdot v \quad (8.2)$$

where  $P$  is the power of QC;  $k$  is the coefficient; and  $v$  is the cargo speed. Then the average consumed power can be shown as (8.3).

$$P_{av} \cdot T_i = \int_0^{T_i} P dt = k \int_0^{T_i} v dt = k \cdot L \quad (8.3)$$

where  $P_{av}$  is the average consumed power of QC;  $T_i$  is the average handling time for one container. Then to handle  $n$  cargos, the consumed time is shown as (8.4).

$$T = n \cdot T_i = kL \sum_{i=1}^n (P_{av})^{-1} \quad (8.4)$$

Generally there exist an upper and a lower limit on the total handling time, i.e.,  $T_{min} \leq T \leq T_{max}$ . Then the demand response model of QC can be obtained.

$$\frac{T_{min}}{kL} \leq \sum_1^n (P_{av})^{-1} \leq \frac{T_{max}}{kL} \quad (8.5)$$

Within the range in (8.5), the consumed power of QCs can be adjusted to facilitate the operation of seaport microgrids.

## References

1. Wilmsmeier, G., Spengler, T.: Energy consumption and container terminal efficiency. Natural Resources and Infrastructure Division, UNECLAC, 2016. <https://repositorio.cepal.org/handle/11362/40928?show=full>
2. MV Ampere. [https://en.wikipedia.org/wiki/MV\\_Ampere](https://en.wikipedia.org/wiki/MV_Ampere)
3. Norled. <https://en.wikipedia.org/wiki/Norled>
4. Clyde puffer. [https://en.wikipedia.org/wiki/Clyde\\_puffer](https://en.wikipedia.org/wiki/Clyde_puffer)
5. Princess Benedikte. <https://www.cruisetimetables.com/cruises-from-copenhagen-denmark.html>
6. The Elektra: Finland's first hybrid-electric ferry. [https://ship.nridigital.com/ship\\_apr18/the\\_elektra\\_finland\\_s\\_first\\_hybrid-electric\\_ferry](https://ship.nridigital.com/ship_apr18/the_elektra_finland_s_first_hybrid-electric_ferry)
7. MF Tycho Brahe. [https://en.wikipedia.org/wiki/MF\\_Tycho\\_Brahe](https://en.wikipedia.org/wiki/MF_Tycho_Brahe)
8. Deep Ocean 01. [http://www.sz.gov.cn/cn/xxgk/zfxxgj/tpxw/content/post\\_8012934.html](http://www.sz.gov.cn/cn/xxgk/zfxxgj/tpxw/content/post_8012934.html)
9. Selbjørnsfjord—Uavpic. <https://uavpic.com/selbjørnsfjord/>
10. SMS Schleswig-Holstein. [https://en.wikipedia.org/wiki/SMS\\_Schleswig-Holstein](https://en.wikipedia.org/wiki/SMS_Schleswig-Holstein)
11. Viking Lady. Available online: <http://maritimeinteriorpoland.com/references/viking-lady/>. Accessed 27 August 2018

12. SF-BREEZE. Available online: <https://energy.sandia.gov/transportation-energy/hydrogen/markettransformation/maritime-fuel-cells/sf-breeze/>. Accessed 27 August 2018
13. Pa-x-ell. Available online: <http://www.e4ships.de/aims-35.html>. Accessed 27 August 2018
14. METHAPU Prototypes Methanol SOFC for Ships. Fuel Cells Bull. 2008, 5, 4–5. 2859(08)70190-1
15. SFC Fuel Cells for US Army, Major Order from German Military. Fuel Cells Bull. 2012, 6, 4
16. Jafarzadeh, S., Schjøberg, I.: Emission reduction in shipping using hydrogen and fuel cells [C]// in Proceedings of the ASME International Conference on Ocean, Offshore and Arctic Engineering, Trondheim, Norway, 25–30 June 2017; p. V010T09A011
17. MS Forester. Available online: <https://shipandbunker.com/news/emea/914341-fuel-cell-technologysuccessfully-tested-on-two-vessels>. Accessed 27 August 2018
18. A Class Submarine. Available online: <http://www.seaforces.org/marint/German-Navy/Submarine/Type-212A-class.htm>. Accessed 27 August 2018
19. SSK S-80 Class Submarine. Available online: <https://www.naval-technology.com/projects/ssk-s-80-classsubmarine/>. Accessed 27 August 2018
20. Kumm, W.H., Lisie, H.L.: Feasibility study of repowering the USCGC VINDICATOR (WMEC-3) with modular diesel fueled direct fuel cells. Arctic Energies Ltd Severna Park MD: Groton, MA, USA (1997)
21. Fan, X., Wang, W., Shi, R., et al.: Analysis and countermeasures of wind power curtailment in China. Renew. Sustain. Energy Rev. **52**, 1429–1436 (2015)
22. Medina, J., Muller, N., Roytelman, I.: Demand response and distribution grid operations: opportunities and challenges. IEEE Transactions on Smart Grid **1**(2), 193–198 (2010)
23. Wang, Y., Pordanjani, I.R., Xu, W.: An event-driven demand response scheme for power system security enhancement. IEEE Trans. Smart Grid **2**(1), 23–29 (2011)
24. Zhao, C., Wang, J., Watson, J.P., et al.: Multi-stage robust unit commitment considering wind and demand response uncertainties. IEEE Trans. Power Syst. **28**(3), 2708–2717 (2013)
25. Kanellos, F.D., Tsekouras, G.J., Hatzigiorgiou, N.D.: Optimal demand-side management and power generation scheduling in an all-electric ship. IEEE Trans. Sustain. Energy **5**(4), 1166–1175 (2014)
26. Lan, H., Wen, S., Hong, Y.Y., et al.: Optimal sizing of hybrid PV/diesel/battery in ship power system. Appl. Energy **158**, 26–34 (2015)
27. Fang, S., Xu, Y., Wen, S., et al.: Data-driven robust coordination of generation and demand-side in photovoltaic integrated all-electric ship microgrids. IEEE Trans. Power Syst. **35**(3), 1783–1795 (2019)
28. Roh, G., Kim, H., Jeon, H., et al.: Fuel consumption and CO<sub>2</sub> emission reductions of ships powered by a fuel-cell-based hybrid power source. J. Marine Sci. Eng. **7**(7), 230 (2019)

**Open Access** This chapter is licensed under the terms of the Creative Commons Attribution-NonCommercial 4.0 International License (<http://creativecommons.org/licenses/by-nc/4.0/>), which permits any noncommercial use, sharing, adaptation, distribution and reproduction in any medium or format, as long as you give appropriate credit to the original author(s) and the source, provide a link to the Creative Commons license and indicate if changes were made.

The images or other third party material in this chapter are included in the chapter's Creative Commons license, unless indicated otherwise in a credit line to the material. If material is not included in the chapter's Creative Commons license and your intended use is not permitted by statutory regulation or exceeds the permitted use, you will need to obtain permission directly from the copyright holder.

